



Influence of 2-naphthoic acid anchoring groups to the photovoltaic performance of zinc phthalocyanine-based photosensitizers in dye-sensitized solar cell

Gülşah Gümrükçü Köse^{a,*}, Gülnur Keser Karaođlan^a, Yaren Erdađ Maden^b, Atif Koca^{b,*}

^a Chemistry Department, University of Yıldız Technical, TR-34220 Esenler, Istanbul, Turkey

^b Chemical Engineering Department, Engineering Faculty, Marmara University, TR-34722 Güztepe, Istanbul, Turkey

ARTICLE INFO

Keywords:

Synthesis
Asymmetric phthalocyanine
Anchoring group
Dye-sensitized solar cell
Electrochemistry
Spectroelectrochemistry

ABSTRACT

Two different zinc phthalocyanines bearing different numbers of 2-naphthoic acid anchoring groups at the peripheral positions were synthesized and characterized with UV–Vis, proton nuclear magnetic resonance (¹H NMR), Fourier transform infrared (FT-IR), and matrix-assisted laser desorption/ionization mass (MALDI-TOF MS) spectroscopy. Then their electrochemical, and spectroelectrochemical performances were investigated to predict their suitability of them as photosensitizers in dye-sensitized solar cells (DSSC). In the voltammetric analysis results, [2,9,16-Tri-(4-carboxyethylphenoxy)-23-(4-[6-carboxy-2-naphthoxy]) substituted zinc(II) phthalocyanine (ZnPc(3)) and [2,9,16,23-tetra-(4-(6-carboxy-2-naphthoxy) substituted zinc(II) phthalocyanine (ZnPc(4)) illustrate similar electron transfer processes. The substituent environments of the complexes slightly influenced the position and reversibility of the redox couples. Redox processes of ZnPc(3) bearing unsymmetrical carboxyethylphenoxy and 2-naphthoic acid anchoring groups slightly shift towards the positive potentials concerning ZnPc(4) bearing symmetrical 2-naphthoic acid substituents. Peak positions of both complexes reflecting the highest occupied molecular orbital (HOMO) and the lowest unoccupied molecular orbital (LUMO) positions indicate the suitability of the complexes for the efficient charge carrier transferring from these photosensitizers to the semiconductor and redox mediator in the DSSC. Pc-based spectroelectrochemical responses of the complexes supported the HOMO and LUMO positions for both neutral and electrogenerated ZnPc species. DSSC responses indicated that ZnPc(3), which has the asymmetric carboxyethylphenoxy and 2-naphthoic acid substituents, gave higher DSSC efficiency with short-circuit photocurrent density (J_{sc}) (9.54 mA cm⁻²), open circuit potential (V_{oc}) (697 mV), fill factor (FF) (51%), incident monochromatic photon-to-current conversion efficiency (IPCE) (51%), and power conversion efficiency (η) (3.4%) parameters concerning ZnPc(4) bearing symmetric 2-naphthoic acid anchoring groups.

1. Introduction

A lot of research is being performed on the production of dye-sensitized solar cells to develop high-yield low-cost devices for use in converting solar energy to electricity [1,2]. A typical DSSC has a nanostructured n-type semiconductor, such as TiO₂, which has a wide band gap, an electrolyte with a redox couple, which is generally I³⁻/I⁻, a counter electrode (CE) to collect the electrons and catalyze the redox couple regeneration, and a sensitizer that absorbs sunlight and produces excitons [3]. The energy levels and the kinetics of electron-transfer events that occur at the interface between the semiconductor surface and the hole-transporting materials of the sensitizer affect the

performance of the DSSC [4]. The dyes can be changed for different kinds of components to enhance the performance of DSSCs, such as porphyrins, metal-free organic dyes, phthalocyanines (Pc), metallophthalocyanines (MPcs), and Ru(II) polypyridyl complexes.

Until now, one of the best efficiency and long-term stability had been achieved by polypyridyl complexes of ruthenium, such as N719 (Industry standard dye (di-tetrabutylammonium *cis*-bis(isothiocyanato) bis(2,2'-bipyridyl-4,4'-dicarboxylato) ruthenium(II)) as the molecular sensitizer [5,6]. However, many of these dyes have some challenges, such as their high cost, environmental incompatibility, and their insufficient light-harvesting properties (their absorption spectra are rather broad, but the NIR absorption is restricted, and the molar extinction

* Corresponding authors.

E-mail addresses: ggumruk@yildiz.edu.tr (G.G. Köse), akoca@marmara.edu.tr (A. Koca).

<https://doi.org/10.1016/j.jelechem.2023.117691>

Received 3 July 2023; Received in revised form 28 July 2023; Accepted 31 July 2023

Available online 1 August 2023

1572-6657/© 2023 Elsevier B.V. All rights reserved.

coefficients are low). Although some Ru-based dyes have improved light-absorption properties in a broad range of the light spectrum through the NIR region such as the black dye (N749) and DX3 (*trans*-dichloro-(dimethylphenylphosphine)-(2,2';6',2''-terpyridyl-4,4',4''-tricarboxylic acid-4-methyl ester)ruthenium(II)) [7], great efforts are concentrated on producing Ru-free sensitizers by using novel organic sensitizers, and particularly porphyrins and phthalocyanines having large conjugated π systems [2,8–10]. MPCs have a wide region of the solar spectrum from UV to IR in terms of light harvesting. It is well reported that the type, number, and location of the substituents, such as peripheral, nonperipheral, or axial, and the symmetric or asymmetric structure of the *Pc* affect their performances in the DSSC application. For instance, according to Urbani et al., at least tetra anchoring groups on symmetrical MPCs increased the strength of the MPCs and the electronic interaction between the dye's LUMO and the Ti 3d orbital. In other studies, although unsymmetrical MPC substitutions can address higher performances, their aggregation is one of the main challenges to be solved to enhance their DSSC performances [11]. Studies on designing new MPC structures as photosensitizers in DSSCs with high performance are continuing intensively to resolve the basic limitations of DSSCs, such as insufficient electron injection efficiency, the hole transport to the electrolyte, the π - π supramolecular interactions (J- or H- aggregates), misappropriateness of the molecular orbitals, adsorption geometry, and orientation of the sensitizers. However, due to extensive studies of MPCs, the reports of DSSC efficiencies of MPCs higher than 3 % are very few [12–14]. Cid, J. J. et al. reported an outstanding IPCE (80 %) and power conversion efficiency (η) (3.52) with ZnPc bearing *tert*-butyl and carboxylic acid substituents at the peripheral positions of *Pc* [14], they proposed that these substituents diminished the aggregation which enhanced the electron and hole transport efficiency. In another paper, 0.57% of η and 4.9% maximal IPCE with a highly substituted zinc phthalocyanine carboxylic acid (ZnPc) was reported by Eu, S. and his coworkers [15]. Giribabu, L. and his coworkers prepared three unsymmetrical zinc phthalocyanines with different numbers and types of substituents to prevent aggregation and reached a maximum of 1.01 % of η with this strategy [16]. Recently to enhance the DSSC performance of various MPCs, we have investigated different MPCs bearing different metal centers, substituents, linkers, and anchoring groups [17,18] and we currently obtained a maximum of 3.97 % η with TiOPc peripherally substituted with tetra-4-carboxyethylenephenoxy [19]. As a continuation of our works so far, now we aim to synthesize new ZnPcs symmetrically substituted with tetra 2-naphthoic acid (ZnPc(4)) and unsymmetrically substituted with one 2-naphthoic acid and three carboxyethylphenoxy anchoring groups (ZnPc(3)). Then we performed detailed electrochemical, spectroelectrochemical, and photovoltaic analyses to represent their DSSC performance to illustrate the influence of the proposed manipulation on the substituent environment of ZnPc on their photovoltaic performances. Although ZnPcs symmetrically substituted with four anchoring groups [19–21] and unsymmetrically substituted with three bulky non-anchoring and one anchoring group [22–24] were extensively studied as dyes in DSSCs, ZnPcs bearing unsymmetrically four anchoring groups are scarce. Thus, the results of this study will provide important scientific output for understanding the effects of the unsymmetrical anchoring groups and naphthoxy and ethylphenoxy spacers between the *Pc* ring and carboxyl anchoring groups on the DSSC performances. It is well documented that in addition to the type, number, and length of the anchoring groups, spacers have significant effects on the DSSC performance. It was well reported in the literature that the molecular engineering of dyes in DSSC further revealed that the high efficiency is not always directly related to the greater steric hindrance. Additionally, the adsorption density of dye on the TiO₂ efficiency surface influences the efficiency as well. It is well documented that the adsorption density of dye could be optimized with the type, number, and length of the anchoring groups and spacers [10]. Since the anchoring group needs to be electronically and strongly connected to the *Pc* ring to improve the electron injection from the LUMO of

the *Pc* to the Ti3d orbital of the TiO₂ [25]. In this aspect, some aromatic linkers, π -conjugated bridges, and vinyl-type conjugated spacers were preferred to improve the strength of the electronic coupling of dyes with TiO₂. Therefore, here we have also investigated the influence of naphthoxy and ethylphenoxy linkers on the overall photovoltaic performance of ZnPcs as dyes in DSSCs.

2. Experimental

2.1. Instruments and chemicals

Commercial suppliers provided all reagents and solvents of reagent-grade quality. The synthesis and purification of 4-(6-carboxy-2-naphthoxy) phthalonitrile (1) and 4-(4-carboxyethylphenoxy) phthalonitrile (2) were carried out as described in the literature [26,18]. Thin-layer chromatography (TLC) (SiO₂) was employed to observe the completion of the reaction. The Perkin Elmer Spectrum One FT-IR (ATR sampling accessory) spectrophotometer was utilized to obtain the FT-IR spectra. A Varian UNITY INOVA 500 MHz instrument was employed to record the ¹H NMR spectra using DMSO-*d*₆ as the solvent. In addition, Agilent 8453 UV/Vis spectrophotometer device was utilized to obtain the UV-Vis spectra. The Bruker Microflex LT MALDI TOF MS was utilized to determine the mass spectra of all the complexes. An Electro-thermal Gallenkamp apparatus was used to measure the melting points of all the obtained compounds. Elemental analyzes were performed with Thermo Flash EA 1112.

2.2. Synthesis and characterization

2.2.1. [2,9,16-Tri-(4-carboxyethylphenoxy)-23-(4-[6-carboxy-2-naphthoxy])-phthalocyaninato zinc(II)] (3)

0.400 g (1.26 mmol) ligand 1, 1.12 g (3.81 mmol) ligand 2, 0.230 g (1.27 mmol) anhydrous Zn(CH₃COOH)₂ and catalytic amount of DBU (1,8-diazabicyclo[4,5,0] undec-7-ene) were added into a closed tube containing 3.0 mL of dimethylformamide (DMF) and mixed in an inert medium at 176 °C. The precipitate formed by adding methanol to the reaction cooled to 25 °C was washed with ethanol, and methanol and dried in a vacuum. The resulting product was purified by column chromatography using 30:1 (v/v) CHCl₃:*n*-hexane (mobile phase). The product shows good solubility in acetone, dichloromethane, tetrahydrofuran (THF), DMF, chloroform, and dimethyl sulfoxide (DMSO). Yield: 115 mg (20%); m.p. > 200 °C. ¹H NMR, DMSO-*d*₆, (δ : ppm): 12.21 (carboxylic acid OH, 4H, s), 7.95–6.60 (Ar-H, 30H, m), 2.94–2.90 (–CH₂, 6H, m), 2.73–2.66 (–CH₂, 6H, m); FT IR $\nu_{\text{max}}/\text{cm}^{-1}$: 3600–2500 (carboxylic acid OH), 3061 (arom. CH), 2941, 2913 (aliph. CH), 1701 (C=O), 1600, 1466 (arom. C=C), 1220 (Ar–O–Ar), 1090, 1043, 945, 866, 822, 745; UV-Vis, DMSO: λ_{max} , nm (log ϵ): 681 (5.09), 614 (4.46), 358 (4.78); Anal. Calc. for C₇₀H₄₆N₈O₁₂Zn: C 66.91, H 3.69, N 8.92, Found: C 66.79, H 3.71, N 8.17%; MALDI TOF MS (*m/z*): Calculated: 1256.55 g/mol; Found: 1279.89 g/mol [M + Na]⁺.

2.2.2. [2,9,16,23-tetra-(4-(6-carboxy-2-naphthoxy))-phthalocyaninato-zinc(II)] (4)

100 mg (0.318 mmol) ligand 3, 15 mg (0.079 mmol) Zn(CH₃COOH)₂, and a catalytic amount of DBU were added into a closed tube containing 1 mL of DMF and mixed in an inert medium at 170 °C. After adding methanol to the reaction mixture cooled to 25 °C, the precipitated phthalocyanine complex was filtered and washed with methanol. The phthalocyanine complex shows good solubility in DMSO and DMF. Yield: 48 mg (46%); m.p. > 200 °C. ¹H NMR, DMSO-*d*₆, (δ : ppm): 13.10 (carboxylic acid OH, 4H, s), 8.71–6.96 (Ar-H, 36H, m); FT IR ν (cm⁻¹): 3600–2500 (carboxylic acid OH), 3063 (arom. CH), 1707 (C=O), 1601, 1468 (arom. C=C), 1216 (Ar–O–Ar), 1146, 1089, 970, 914; UV-Vis, DMSO: λ_{max} , nm (log ϵ): 680 (5.08), 618 (4.42), 354 (4.82); Anal. Calc. for C₇₆H₄₀N₈O₁₂Zn: C 69.02, N 8.47, H 3.05%; found: C 69.56, N 8.09, H 3.61%; MALDI TOF MS (*m/z*): Calculated: 1322; Found: 1322 [M]⁺.

2.3. Electrochemical, in situ spectroelectrochemical, and photovoltaic measurements

All measurements were carried out with a Gamry Reference 600 potentiostat/Galvanostat/ZRA by following the procedure given in the literature [27] in a conventional three-electrode cell consisting of a glassy carbon working electrode (GCE), a Pt wire counter electrode, and an Ag/AgCl reference electrode in 0.10 mol dm⁻³ tetrabutylammonium perchloride (TBAP)/DMSO electrolyte at 25 °C.

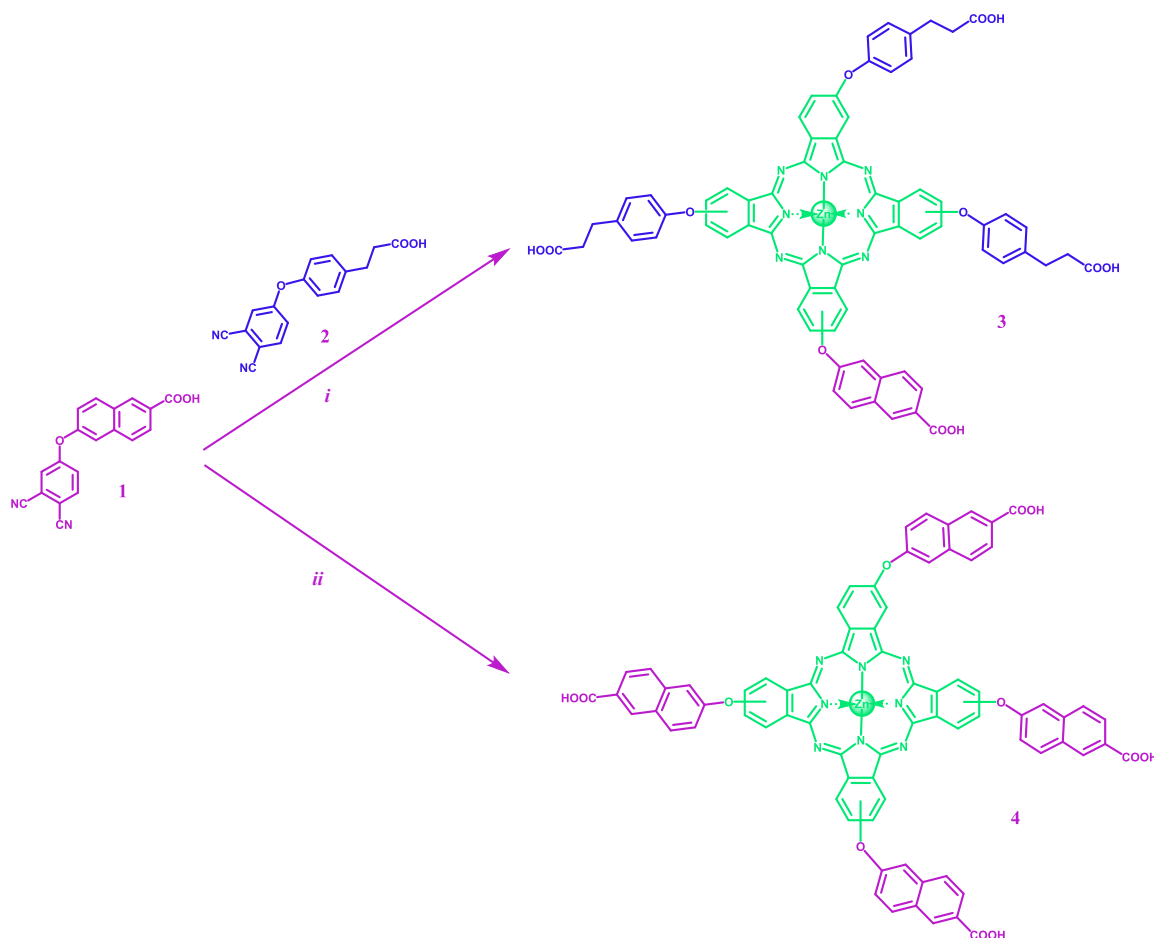
DSSC measurements were performed by following our previous research [18]. In briefly, firstly fluorine doped tin oxide (FTO) coated glass substrates were used as the electrode substrates which were cleaned gently with a soap solution, ethanol, and then distilled water by the sonication and finally dried at 100 °C. Then a TiO₂ paste was applied onto the FTO substrate (active square area: 5 × 5 mm²) using the doctor blade coater to form TiO₂ film with well defined thickness. The sharp blade of the coater was kept 25 μm away from the surface of the FTO substrate. FTO substrates were pre-heated at 120 °C for 15 min to vaporize the solvent inside of the paste. The films are then heated from 120 to 450 °C at a continuous rate of 5 °C/min, and the temperature remains constant for the next 30 min. The coating process was repeated with the opaque TiO₂ paste, and the film was calcined again. The TiO₂ photoanode was immersed in the 40.0 mM TiCl₄ aqueous solution for 30 min at 70 °C, and the last calcination process was done for 30 min at 450 °C. Finally, the TiO₂ photoanodes were then immersed in 0.4 mM ZnPc (3) and (4) DMSO solutions for 24 h. The amounts of the adsorped dyes were calculated by measuring the UV-Vis spectra of the ZnPc/DMSO solution. Similarly possible desorption of the adsorped ZnPcs on the electrode surface was tested by keeping the modified electrodes in

acetonitrile and the amount of ZnPc in solution was tested with UV-Vis spectral measurements. Chenodeoxycholic acid (CDCA) was also introduced into the dye solution as a coadsorbent with a 10-fold concentration of the dye. Pt counter electrodes were formed on FTO substrates by casting a platinum paste solution and sintered for 15 min at 420 °C. A sandwiching cell structure was constructed by using the spacer between the electrodes. The redox electrolyte, which is Iodolyte AN-50 liquid, was injected between the counter and the working electrodes. Iodolyte AN-50 liquid is a low-viscosity electrolyte formulated by Solaronix for high-performance DSSCs. This electrolyte consists of iodine/tir-iodide, ionic liquid, lithium salt, pyridine derivatives, and acetonitrile. The photocurrents and photovoltage responses of the DSSCs were measured by using a HAL-320 Asahi solar simulator equipped with a 300 W xenon lamp, The solar simulator was calibrated under global standard air mass (AM 1.5, 100 mW cm⁻²) condition by employing KG5 filtered Si reference solar cell.

3. Results and discussion

3.1. Synthesis and characterization

Asymmetric phthalocyanines exhibit various properties because they contain different substituents. For this purpose, in our study, a new A₃B type asymmetric zinc (II) phthalocyanine (3) containing 6-carboxy-2-naphtoxy and 4-carboxyethylphenoxy groups was synthesized in the presence of DBU at 170 °C in an argon atmosphere using the statistical cyclotetramerization method with 20% yield. In addition, the symmetric zinc(II) phthalocyanine (4) complex was obtained in 46% yield by reacting the 6-carboxy-2-naphtoxy phthalonitrile derivative with Zn



Scheme 1. The synthesis of ZnPcs(3–4). (i) K₂CO₃, DMF, 75 °C; (ii) metal salts, DBU, DMF, 24 h and 170 °C.

(CH₃COOH)₂ at 170 °C in the presence of DBU in an argon atmosphere using the procedure described in the literature [19] (Scheme 1).

The results obtained from elemental analysis, MALDI TOF MS, ¹H NMR, FTIR, and UV-Vis spectroscopic methods used to elucidate the structures of all synthesized complexes show that the structures were successfully synthesized (Figs. S1–S6). First of all, when the FTIR spectra are examined, the absence of C=N peaks at 2232 cm⁻¹ of the ligands proves the formation of these phthalocyanine complexes. Peaks of carboxylic acid –OH groups were observed at 2500–3600 cm⁻¹, while –C=O groups of complexes ZnPc(3) and (4) were observed at 1701 and 1707 cm⁻¹, respectively. Aliphatic peaks of complex ZnPc(3) were observed just below 3000 cm⁻¹, while aromatic peaks of complexes ZnPc(3) and (4) were observed just above 3000 cm⁻¹. Ar–O–Ar peaks appeared at 1220 and 1216 cm⁻¹, and aromatic C=C peaks at 1600, 1466, 1601, and 1468 cm⁻¹, respectively.

When the ¹H NMR spectra of compounds ZnPc(3) and ZnPc(4) taken in d₆-DMSO were examined, the aromatic system protons of these compounds were observed as a multiplet at δ 7.95–6.60 ppm for complex ZnPc(3) and δ 8.64–7.38 ppm for complex ZnPc(4). Protons belonging to the carboxylic acid group appeared as a singlet at δ 12.21 and δ 13.10 ppm, respectively. The aliphatic protons belonging to each –CH₂ group appeared as multiplet at δ 2.94–2.90 and δ 2.73–2.66 ppm in the ¹H NMR spectrum of ZnPc(3).

UV-Vis spectroscopy technique is indispensable to investigate the structure and behavior of phthalocyanine macrocyclic compounds in solutions. The Soret (B) band, which is around 300–350 nm in the UV region of the electronic absorption spectrum, and the Q band, which is between 600 and 800 nm in the UV-Vis region and is observed due to π-π* transitions from the highest occupied molecular orbital (HOMO) to the lowest unoccupied molecular orbital (LUMO), are the two characteristic bands of metallophthalocyanine complexes. UV-Vis absorption spectra of asymmetric ZnPc(3) and symmetric ZnPc(4) phthalocyanines in DMSO are shown in Fig. 1. The intensive low-energy Q-bands of complexes ZnPc(3) and (4) were observed at 681 nm and 680 nm with satellite bands at 614 nm and 618 nm in turn while high-energy B-bands were seen at 358 nm and 354 nm, respectively.

The strong interaction between the transition dipole moments of the Pc molecules causes these molecules to be stacked side by side (J type) or one under the other (H type) in dimeric or oligomeric structures in solution. This phenomenon, known as aggregation, varies with temperature, concentration, solvent, core metal, and substituents in peripheral regions. They also cause the broadening of the electronic absorption bands in the UV-Vis spectra of phthalocyanines. In the UV-VIS absorption spectrum, H-type aggregation causes a hypsochromic shift in

the Q band, while J-type aggregation causes a bathochromic shift.

Complexes ZnPc(3) and ZnPc(4) were examined for their aggregation behaviors in DMSO within the concentration range of (2.0–12.0) × 10⁻⁶ M (Fig. 2). The successful sensitization of the material necessitates the non-existence of aggregation in the solution, as the occurrence of aggregation presents difficulties in the practical utilization of phthalocyanines. Elevation of concentration led the Q band intensity to increase harmoniously without any shift, indicating the absence of complex aggregation. ZnPc(3) and ZnPc(4) were found to adhere to Lambert Beer's law and exhibited no signs of aggregation in DMSO. The aggregation of MPcs was generally diminished by using bulky substituents, such as tert-butyl groups [28]. However, many other factors influence the aggregations, such as dimerization constants, solvents, substituent type numbers and positions, the coordination number of central metals, and axial substitutions. There are many strategies to prevent the aggregation of MPcs in addition to using bulky substituents. It is well documented that the substitutions of MPcs with benzene-containing groups at the β positions suppresses the aggregation by the rigid steric orientation of benzo groups above and below the Pc ring [28,29]. Here, 2-naphthoic acid and carboxyethylphenoxy groups of ZnPc(3) and ZnPc(4) most probably diminish the aggregation in DMSO.

In the mass spectrum of compounds ZnPc(3) and ZnPc(4), presence of the molecular ion peaks at *m/z* = 1279 [M + Na]⁺ and 1322 [M]⁺ respectively, displays the formation of the proposed structures.

3.2. Voltammetric measurements

CV curves of ZnPc(3) and ZnPc(4) are one of significant indicators for critiquing the usability of them in the DSSC area. Table 1 displays the half-wave peak potentials (*E*_{1/2}) of the complexes' redox reactions derived from their voltammograms in Fig. 3 and Fig. 4. Because of the inactivity of the Zn²⁺ cation in the core of these compounds, both ZnPc(3) and ZnPc(4) only display Pc ring assigned redox activity.

As shown in Fig. 3, two reversible and one quasi-reversible reduction couples are recorded at -0.72 V (Red(1)), -1.37 V (Red(2)), and -2.53 V (Red(3)) with ZnPc(3). The electrochemical reversibility of Red(1) and Red(2) couples are confirmed with their peak potential separations (Δ*E*_p) and peak current ratios (*I*_{pa}/*I*_{pc}). In addition to the reduction processes, one quasi-reversible oxidation wave is recorded at about 0.72 V (Oxd(1)) during the positive potential scans. It is well known that the peak potentials are directly related to the energy levels of the HOMO and LUMO positions of the Pc ring, thus HOMO and LUMO values are derived as -3.50 and -5.00 eV respectively. When the unsymmetrical substituent environment is converted to a symmetric structure by

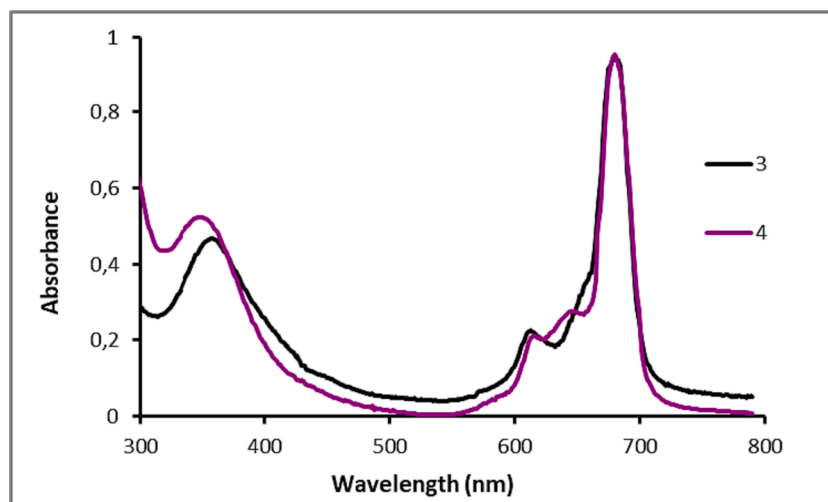


Fig. 1. UV-Vis spectra of complexes ZnPc(3) and ZnPc(4) in DMSO.

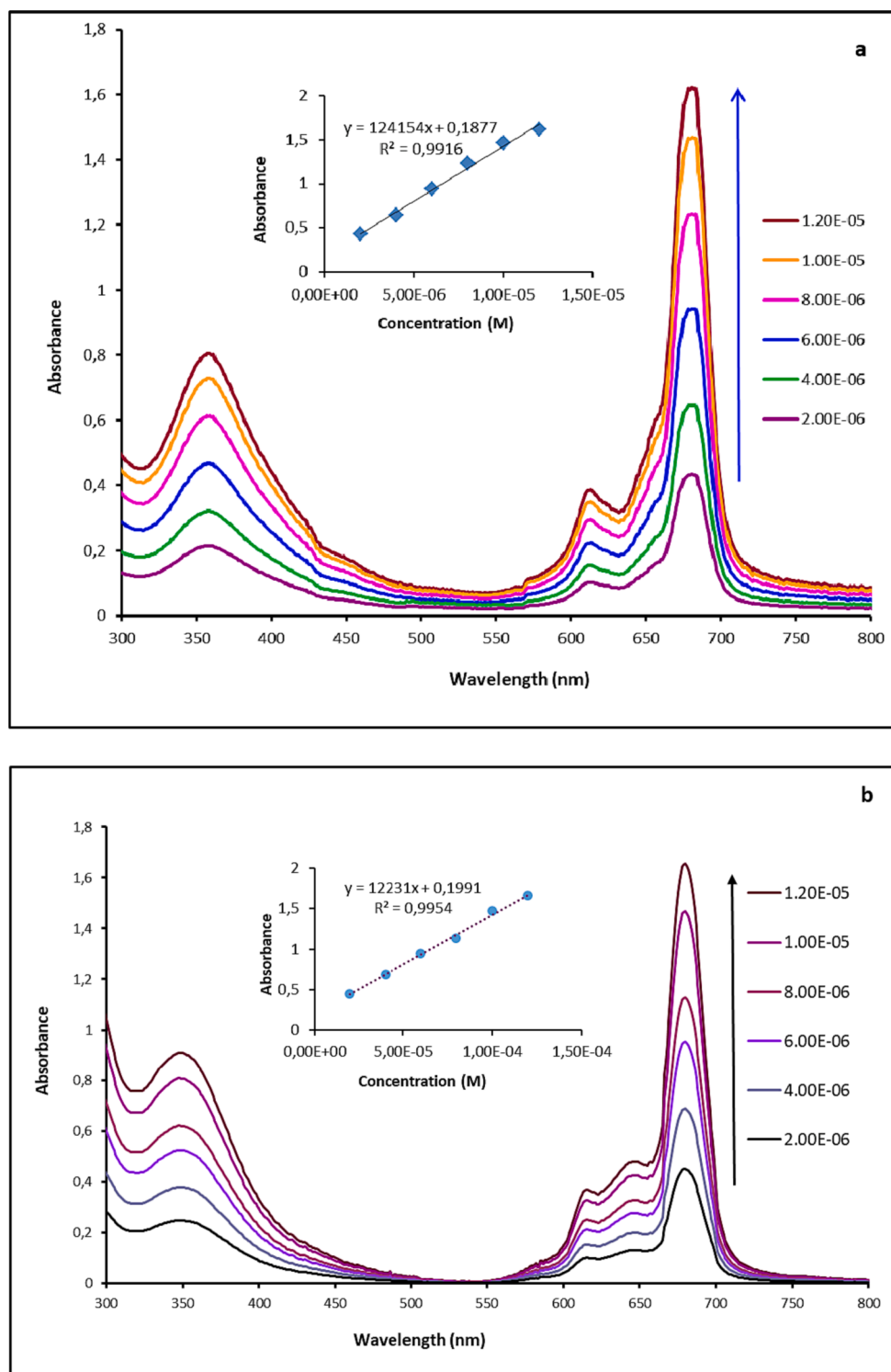


Fig. 2. UV-Vis absorption spectra of a) ZnPc(3) and b) ZnPc(4) in DMSO at varying concentrations.

changing three carboxyethylphenoxy groups with 2-naphthoic acid ones (ZnPc(4)), redox processes shift towards the positive potentials, and three reductions and one oxidation peak were observed at -0.80 V (Red (1)), -1.16 V (Red (2)), -1.42 V (Red (3)) and 0.91 V (Oxd(1)) respectively (Fig. 4). These potential shifts cause to the shifting of HOMO and LUMO positions to -3.40 and -5.20 eV respectively for ZnPc(4). When with the conduction band (CB) and valance band (VB) of TiO_2 semiconductors and the reduction potential of the mediator of DSSCs are considered, both ZnPc complexes have suitable band

positions for the efficient electron transport from LUMO of the ZnPc to CB of TiO_2 and the hole transport from the mediator to the HOMO of ZnPc.

3.3. In-situ spectroelectrochemical measurements

In-situ spectroelectrochemistry technique is a potent characterization method that combines the benefits of both conventional electrochemistry and spectroscopy. Spectroscopic information such as light

Table 1

Electrochemical data of the complexes in DMSO/TBAP solution. All potentials were given versus Ag/AgCl.

Complexes	Red(1) (V)	Red(2) (V)	Red(3) (V)	Oxd(1) (V)	^a E _{LUMO} (eV)	^b E _{HOMO} (eV)	^c E _{gap} ^{red} (eV)	^d E _{gap} ^{opt} (eV)	Ref.
^e ZnPc	-0.86	-1.10	-	0.76	-3.47	-4.95	1.48		[18]
^f CoPc	-0.41	-1.28	-1.87	0.19	-3.92	-4.52	0.60		[18]
^g ZnPc	-1.08	-1.56	-	0.55			1.63		[30]
^h ZnPc	-0.82	-1.32	-	0.75			1.57		[30]
ⁱ ZnPc	-0.95	-	-	0.58	-3.45	-4.98	1.53		[31]
^j ZnPc	-1.38	-	-	0.54	-3.53	-5.25		1.72	[22]
ZnPc(3)	-0.72	-1.37	-2.53	0.72	-3.28	-5.05	1.44	1.77	tw
ZnPc(4)	-0.80	-1.16	-1.42	0.91	-3.38	-5.13	1.71	1.75	tw

^a : E_{HOMO} (eV) = -E_{Oxd(1)} + E_{1/2} (Fc/Fc⁺) - IP (Fc) [32,33]. ^b: E_{LUMO} = E_{gap}^{opt} (eV) + E_{HOMO} (eV) [32]. ^c: E_{gap} = |E_{Oxd(1)}| + |E_{Red(1)}| in eV. ^d E_{gap}^{opt} (eV) = $\frac{hc}{\lambda_{onset}} = \frac{1240(eV)}{\lambda_{onset}}$. [E_{1/2} (Fc/Fc⁺) = 0.47 V vs. Ag/AgCl. IP(Fc) 4.8 eV. Fc = ferrocene].

^e: peripherally tetra-4-carboxyethylphenoxy substituted zinc(II) phthalocyanine. ^f: peripherally tetra-4-carboxyethylphenoxy substituted cobalt(II) phthalocyanine. ^g: mono-*tert*-butylphenoxy substituted zinc(II) phthalocyanine. ^h: three-*tert*-butylphenoxy substituted zinc(II) phthalocyanine. ⁱ: three-*tert*-butylphenoxy and one catechol substituted zinc(II) phthalocyanine. ^j: ZnPc bearing tribenzonaphtho-condensed porphyrine with one carboxyl and three *tert*-butyl substituents.

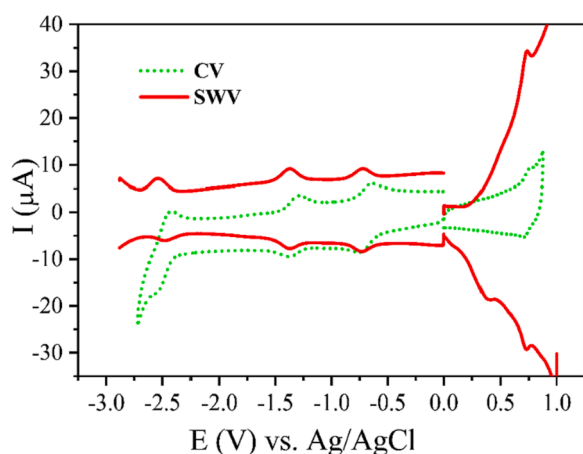


Fig. 3. CVs and SWVs of ZnPc(3) (5.0×10^{-4} mol dm⁻³) on a GCE in DMSO/TBAP.

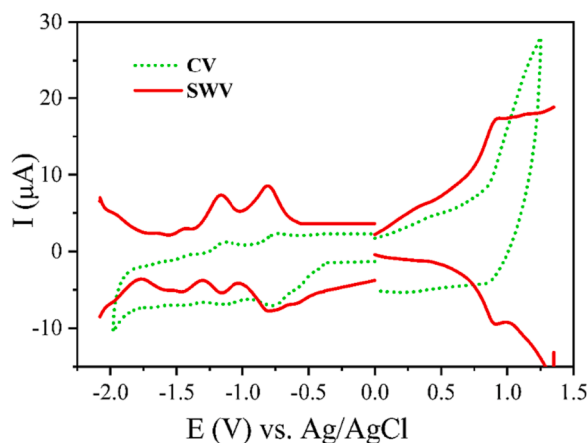


Fig. 4. CVs and SWVs of ZnPc(4) (5.0×10^{-4} mol dm⁻³) on a GCE in DMSO/TBAP.

emission and scattering, electronic absorption, and vibrational frequencies of in situ electrochemically created redox-active species can be collected at various potentials [34]. Additionally, in-situ spectroelectrochemical data information about the peak assignments and altering energy levels with potential excitations. Thus, in-situ spectroelectrochemical measurements of ZnPc(3) and ZnPc(4) are carried out to

predict the origin of the electron transfer reactions and to investigate the influences of the redox processes on the band energy levels of the moieties. It is observed that ZnPc complexes display very similar UV-vis spectral responses during the in situ spectroelectrochemical measurements, which shows that altering the substituents on the Pc core does not affect their spectral changes during the electron transfer reactions. In situ UV-vis spectra change of the ZnPc(3) is given as an example (Fig. 5). The B and Q bands of ZnPc(3) are observed at 350 and 680 nm for the neutral species, respectively. As shown in Fig. 5a and b, the Q band decreases without a shift while new bands are observed at the ligand-to-metal charge transfer (LMCT) regions. These spectral changes indicate that [Zn^{II}Pc⁻²] is reduced to [Zn^{II}Pc⁻³]⁻¹ species during the first reduction reaction. Similarly, [Zn^{II}Pc⁻³]⁻¹ species reduce to dianionic [Zn^{II}Pc⁻⁴]⁻² species during the second reduction reaction. Decreasing the Q bands without a shift in the wavelength represents that the addition of electrons to the LUMO of the Pc ring does not change the energy level of the LUMO orbitals while decreasing the molar excitation coefficient for the electrogenerated monoanionic [Zn^{II}Pc⁻³]⁻¹ and dianionic [Zn^{II}Pc⁻⁴]⁻² species [35–37]. During the oxidation process under the 1.00 V applied potential, all bands decrease in intensity, which is also a characteristic change for the formation of [Zn^{II}Pc⁻¹]⁺¹ species and their decomposition under applied potential (Fig. 5c). In Fig. 5d, each icon (Δ, ○, □, *) in the chromaticity diagram represents the color of the neutral, anionic, and cationic species, [Zn^{II}Pc⁻²], [Zn^{II}Pc⁻³]⁻¹, [Zn^{II}Pc⁻⁴]⁻², [Zn^{II}Pc⁻¹]⁺¹ respectively.

3.4. Photovoltaic measurements

The photoinduced charge separation at the TiO₂/dye/electrolyte interface and transferring of the electrons from the LUMO of the dye to CB of TiO₂ and hole transferring from the HOMO of dye to the mediators in the electrolyte are the key factors for the efficiency of the DSSCs. When these charge transfer processes do not happen very fast, recombination reactions take place, resulting in a lower photoconversion efficiency for the device [38]. At this point, band gaps of the semiconductors and HOMO-LUMO positions are at the forefront of the engineering work that needs to be done to ensure the suitability of the dye in these devices. The HOMO level and the LUMO level of ZnPc(3) and ZnPc(4) complexes are derived from the first oxidation and first reduction processes recorded with CV and SWV analyses. HOMO-LUMO positions listed in Table 1 indicate the applicability of both ZnPcs as photosensitizers in DSSC applications. The LUMO energy level of the sensitizer should be higher than the CB of TiO₂ to ensure effective electron injection and the HOMO level should be lower than the redox potential of the electrolyte (-4.75 eV) [38].

To investigate the PV performances of the ZnPc complexes, FTO/

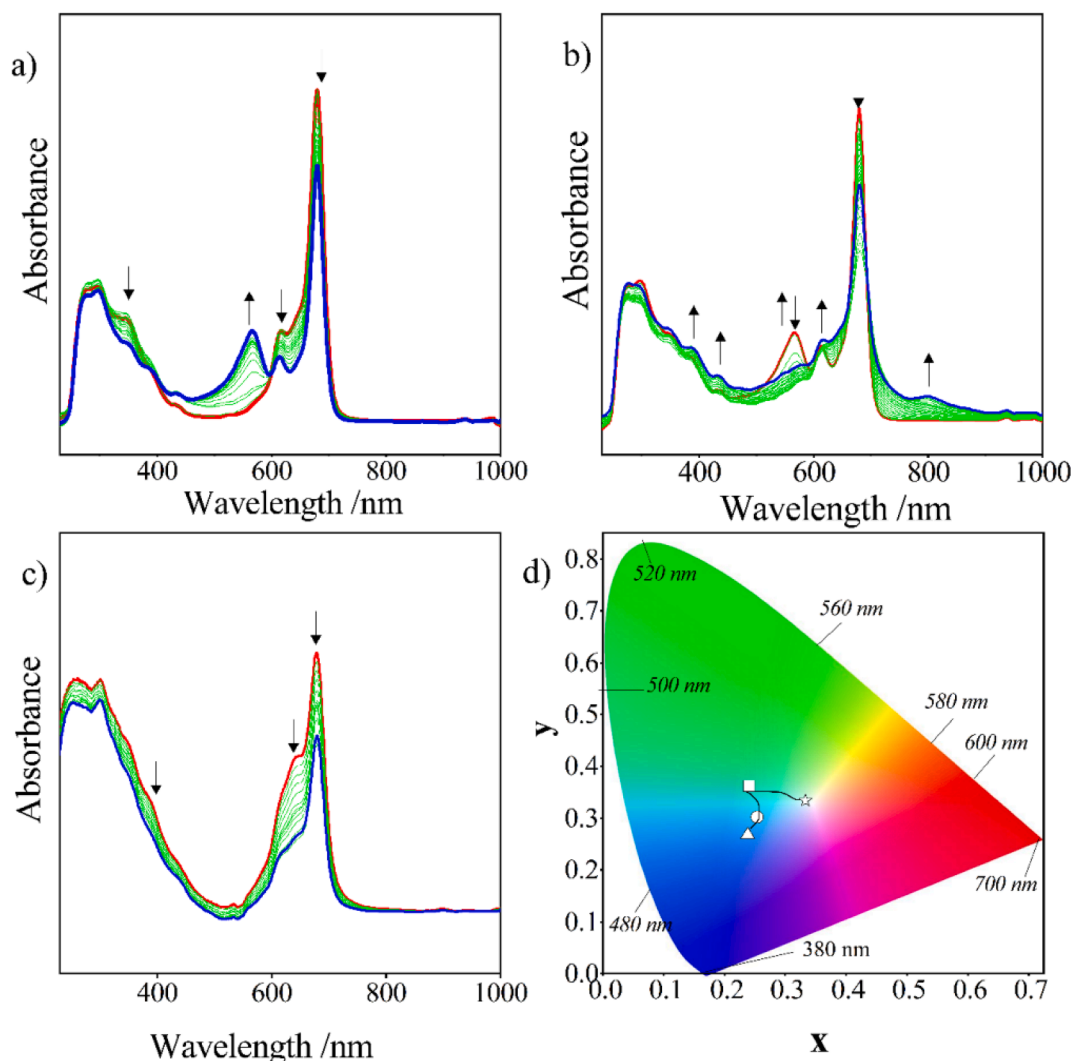


Fig. 5. In-situ UV-Vis spectra of ZnPc(3) in DMSO/TBAP electrolyte. a) $E_{app} = -0.7$ V, b) $E_{app} = -1.1$ V, and c) $E_{app} = 1.0$ V. (Red spectrum: initial response before the corresponding potential application. Blue spectrum: final response after the corresponding potential application. Green spectra: the responses during the corresponding redox reaction). d) Chromaticity diagram; \square : $[Zn^{II}Pc^{2-}]$; \circ : $[Zn^{II}Pc^{3-}]^{-1}$; \triangle : $[Zn^{II}Pc^{4-}]^{2-}$; $*$: $[Zn^{II}Pc^{1-}]^{1+}$.

TiO₂/ZnPc(3) and FTO/TiO₂/ZnPc(4) photoelectrodes are prepared by adsorption of the ZnPcs from their DMSO solutions. The amount of the adsorbed ZnPc(3) and ZnPc(4) are found as 3.4×10^{-11} and 1.3×10^{-11} mol on the 1.0 cm² surface area of the FTO/TiO₂ electrode for ZnPc(3) and ZnPc(4) respectively. The less ZnPc(4) dye loading may result from the bulkier structure of the 2-naphthoic acid anchoring groups concerning the carboxyethylphenoxy substituents on the ZnPc(3). After preparations of FTO/TiO₂/ZnPc(3) and FTO/TiO₂/ZnPc(4) photoelectrodes, the DSSC structures are constructed as FTO/TiO₂/ZnPc/electrolyte/Pt/ITO devices and their photovoltaic performances are determined by examining the current density–voltage (J–V) and electrochemical impedance spectrum (EIS) responses. Open circuit potential (V_{OC}), short-circuit photocurrent density (J_{SC}), FF values, and overall power conversion efficiencies (η) of the DSSC were listed in Table 2 as the fundamental parameters.

As shown in Fig. 6, the photovoltaic performance of ZnPc(3) is considerably higher than that of ZnPc(4) under a standard AM 1.5 illumination condition. While ZnPc(3) has 9.54 mAcm^{-2} of J_{SC} , 697 mV of V_{OC} , 51 of FF, and 3.40 η , these values decrease to 9.01, 564, 34, and 1.72 respectively. As shown in Table 2, the photovoltaic performance of ZnPc(3) is higher than that of the ZnPcs reported in the literature. The designing ZnPc(3) with one naphthoxy and three ethylphenoxy linkers and four carboxy anchoring groups facilitate

Table 2
Photovoltaic properties of the MPC bearing DSSCs.

Dye	J_{SC} (mA/cm ²)	V_{OC} (mV)	FF (%)	η (%)	IPCE (%)	Ref.
^a TiOPc	11.72	466	60.8	3.32	68	[18]
^a CoPc	8.47	370	11.6	1.02	52	[18]
^a ZnPc	9.36	428	24.4	2.20	48	[18]
^a H ₂ Pc	10.98	471	56.4	2.92	37	[18]
^b ZnPc	5.9	662	76	2.95		[39]
^c ZnPc	7.0	634	74	3.20		[39]
^d ZnPc	0.555	375	45	0.37		[40]
^e ZnPc	0.466	486.75	55	0.50		[40]
^f ZnPc	6.16	750	53	2.45	46	[41]
^g ZnPc	4.80	610	74	2.20	44	[14]
N719	19.10	721	66.4	9.14	85	tw
ZnPc(3)	9.54	697	51	3.40	51	tw
ZnPc(4)	9.01	564	34	1.72	47	tw

^a: Pc ring was substituted with peripheral tetra-4-carboxyethylphenoxy groups. ^b: ZnPc tetra substituted with three *tert*-butyl and one carboxy group. ^c: ZnPc substituted with three *tert*-butyl and two carboxy groups. ^d: ZnPc substituted with tetra carboxy groups. ^e: ZnPc substituted with tetra sulfoxy groups. ^f: ZnPc with *hexa*-tertiary substituted carbazolyl donor groups and one carboxylic acid anchoring group. ^g: Pc with three *tert*-butyl electron-donating and one benzoic acid anchoring group.

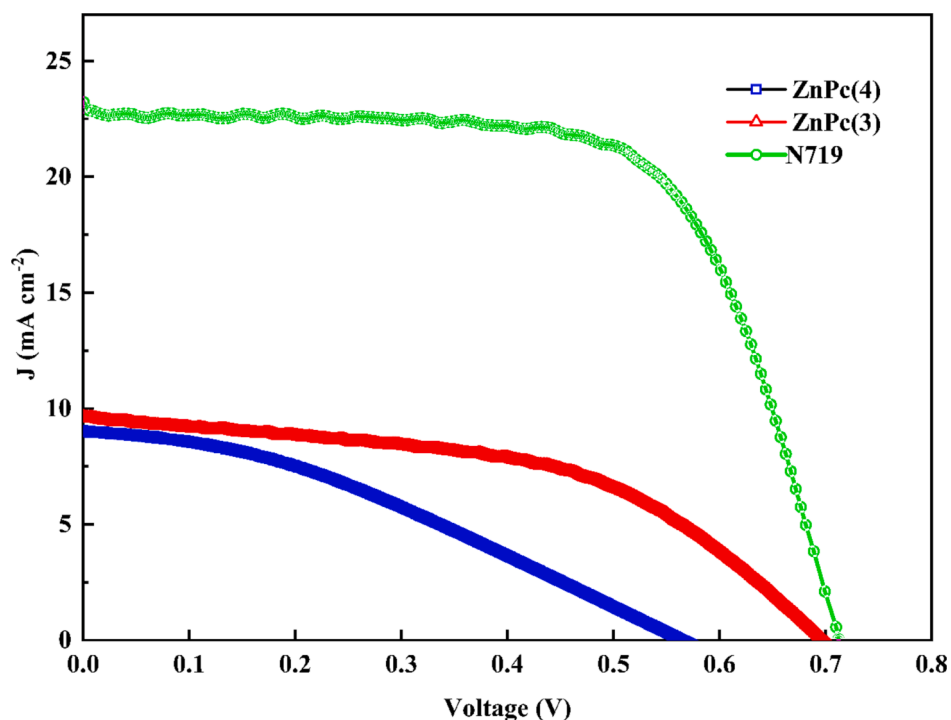


Fig. 6. J–V curves of the ZnPc (3) and ZnPc (4).

the charge transfer ability of the dye concerning the ZnPcs having unsymmetrically substituted with three bulky groups and one anchoring one or bearing four symmetric same spacer and anchoring groups [18,39–41].

The ratio between the number of generated electrons and the number of incident photons, the incident photon-to-current conversion efficiency (IPCE), is obtained (Fig. 7). As a support for the J–V responses, at $\lambda = 520$ nm, ZnPc(3) and ZnPc(4) have 51% and 47% IPCE values,

respectively.

The photovoltaic performance of ZnPc(3) and (4) are also examined with the EIS analysis. The EIS is a powerful tool for better understanding the electrical and ionic transport processes in DSSCs [39]. It was performed with a potentiostat and a solar simulator, and it was obtained in the frequency range of 10 mHz to 1 MHz with an intensity of 1000 W/cm² and a perturbation of 10 mV under standard illumination of AM1.5G. To estimate the lifetimes and conductivities of DSSCs, the

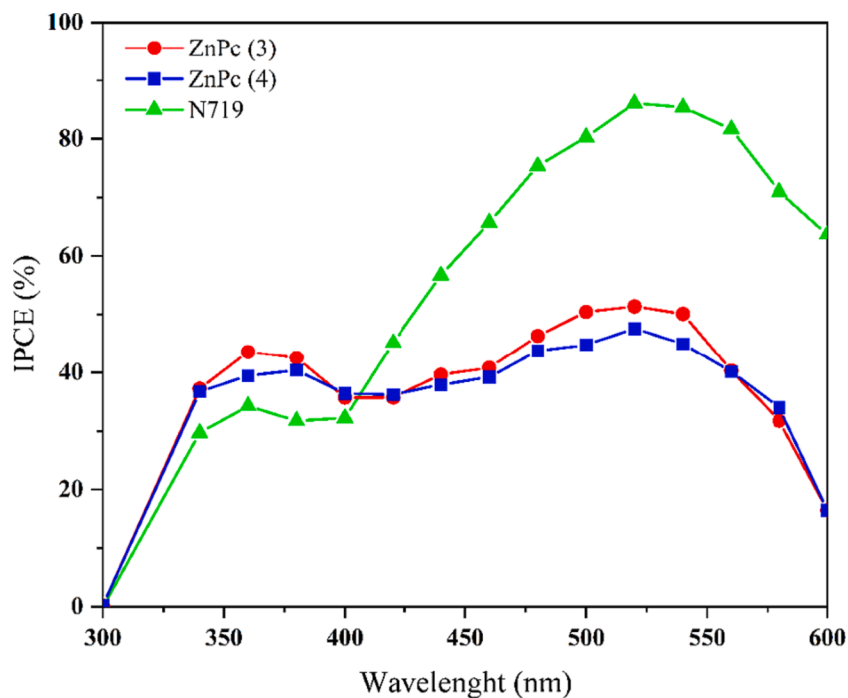


Fig. 7. IPCE values of the ZnPc(3), ZnPc(4), and N719 (Industry standard dye (di-tetrabutylammonium *cis*-bis(isothiocyanato)bis(2,2'-bipyridyl-4,4'-dicarboxylato) ruthenium(II)).

Nyquist plots (Fig. 8a) and Bode plots (Fig. 8b) are fitted into the equivalent circuit in the inset of Fig. 8b. ZnPc(3) and (4) have the two semicircles in Nyquist plots (Fig. 8a). The starting point of the plots is represented by R_s , which is the resistance of the FTO. The small loop in the high-frequency region is R_{PT} , and it is the resistance of the electron interface, which consists of the counter electrode and electrolyte interface. Also, the large loop in the low-frequency region is R_{CT} represents the resistance of the TiO_2 /dye/electrolyte couple interfaces [39]. As a result, the varying values of R_{CT} provide some useful information regarding the electrodes' recombination kinetics. The smaller R_{CT} means a faster electron transfer kinetics [39]. The photovoltaic performance relation (Table 2) between the ZnPc(3) and (4) is consistent with the charge transfer resistance performance (Table 3).

Electron lifetime (τ_e), which is the other important parameter of the performance of the electrodes, can be calculated with the maximum frequency value (Fig. 8b) and with the $\tau_e = 1/2\pi f_{max}$ equation [42]. The electron lifetime of the ZnPc(3) and ZnPc(4) are calculated as 0.72 ms, and 0.34 ms respectively. High electron lifetime leads to improved electron transfer efficiency, which increases the photovoltaic efficiency of solar cells. As a result, EIS analysis demonstrates that asymmetric ZnPc(3) can enhance electron transport while limiting charge recombination, hence enhancing the J_{SC} and power conversion efficiency of DSSCs. Different charge recombination features of ZnPc(3) and ZnPc(4) may have resulted from different substituents on these complexes. It is well documented that the Pc ring which has donor properties, can be readily doped by electron-accepting substituents, due to the forming of donor-acceptor structure [43]. Substituents on the MPCs have a significant effect on their aggregation of them, charge transfer rate, absorption strength, push-pull effect, and orientation of them on the surface and all these features influence their performance [43–45]. Most probably, altering three 2-naphthoic acid groups with carboxyethylphenoxy anchoring groups improve the push-pull effect of the dye, thus ZnPc(3) has better electron injection features than the TiO_2 semiconductor concerning symmetrically substituted ZnPc(4). Altering the substituents on ZnPc(3) and ZnPc(4) may also influence the arrangement of the excited states by permitting directionality on the charge transfer from the LUMO orbital of them to the conduction band of TiO_2 and, therefore, optimizing the photovoltaic performance of the DSSCs [43].

Due to the improvements of the charge recombination with the better push-pull effect, ZnPc(3) has long electron lifetime than ZnPc(4). ZnPc(3) bearing unsymmetrically three 2-naphthoic acids and one carboxyethylphenoxy anchoring group has better photovoltaic

Table 3

DSSC equivalent circuit parameters determined via electrochemical impedance spectroscopy.

Dye	$R_s(\Omega)$	$R_{PT}(\Omega)$	$R_{CT}(\Omega)$	$f_{max}(\text{Hz})$	$\tau_e(\text{ms})$
ZnPc(3)	43.2	97.0	511.9	208.3	0.76
ZnPc(4)	50.1	84.48	539.65	467.9	0.34
N719	9.72	19.07	15.58	196.64	0.81

performance than the ZnPc containing tetra-4-carboxyethylenephenoxy anchoring groups (11.28 of J_{SC} (mA/cm^2), 470 of V_{OC} (mV), 54.6 of FF (%), and 2.89 of η (%)) [19], which supports the enhancement of push-pull effects of the modification of ZnPc with four unsymmetrical anchoring groups.

In the evaluation of the performance of the DSSC, stability is as important a parameter as efficiency. Components of the DSSC, which are the substrate (conductive substrate or conductive film-coated substrate), semiconductor nanostructure (photoanode), sensitizer (dye), electrolyte, and catalyst-coated counter electrode, affect the total stability of the cell. To obtain the stability performance of the ZnPc(3) and (4), LSV and EIS analyses were performed on 50 trials at 25 °C and under the 1 sun light soaking. The performances of ZnPc(3) and (4) were impressively steady and did not change after 50 LSV excitations, as illustrated in Figs. 9 and 10.

4. Conclusion

Two ZnPcs, asymmetric ZnPc(3) bearing one naphthoxy and three ethylphenoxy linkers and four carboxy anchoring groups and symmetric ZnPc(4) bearing tetra ethylphenoxy linkers between four carboxy anchoring groups and Pc core were synthesized as the photosensitizers for the DSSCs in this work. Decorating the complexes with benzene-bearing spacers at the substituents suppress the aggregation of both complexes, which is one of the main parameters for their applications of them as dyes in DSSCs. Voltammetric and spectroelectrochemical analyses were performed to forecast their potential usage capabilities on the DSSC applications. In the UV-Vis region, both complexes showed unique B and Q bands with high molar extinction coefficients. According to the reduction and oxidation process peak analyses, HOMO and LUMO levels of both species are suitable for usage in DSSC with a TiO_2 photoanode. According to the LSV analyses, ZnPc(3) has a higher performance than the ZnPc(4) with J_{SC} of 9.54 mA cm^{-2} , a V_{OC} of 697 mV, a FF of 51%,

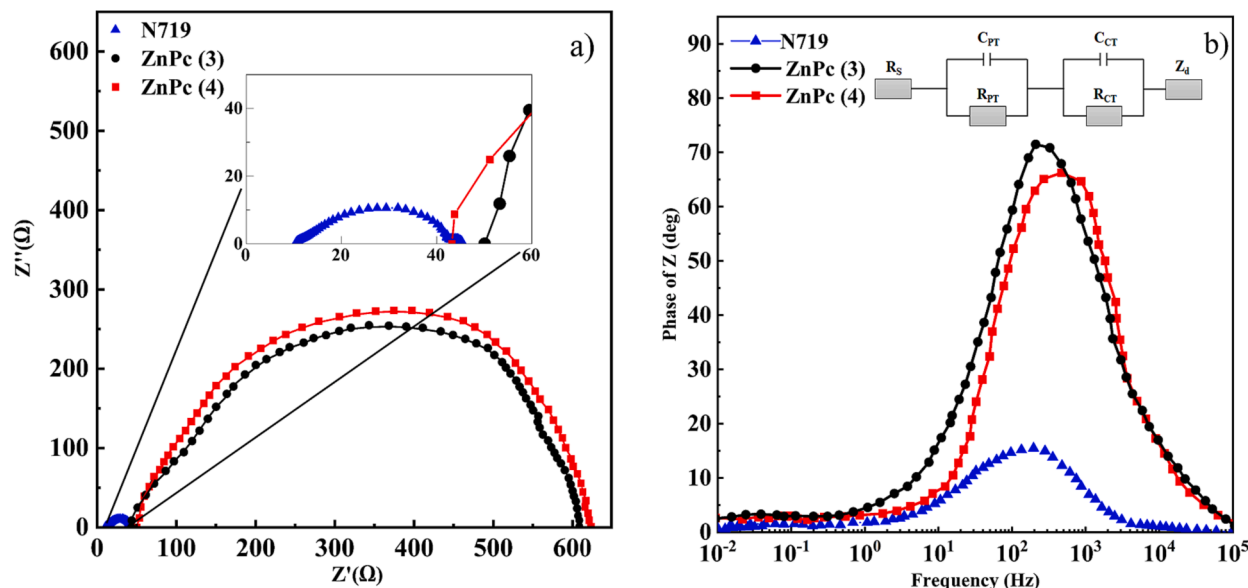


Fig. 8. A) nyquist plots and b) bode plots from the eis analysis of the ZnPc (3), ZnPc (4), and N719.

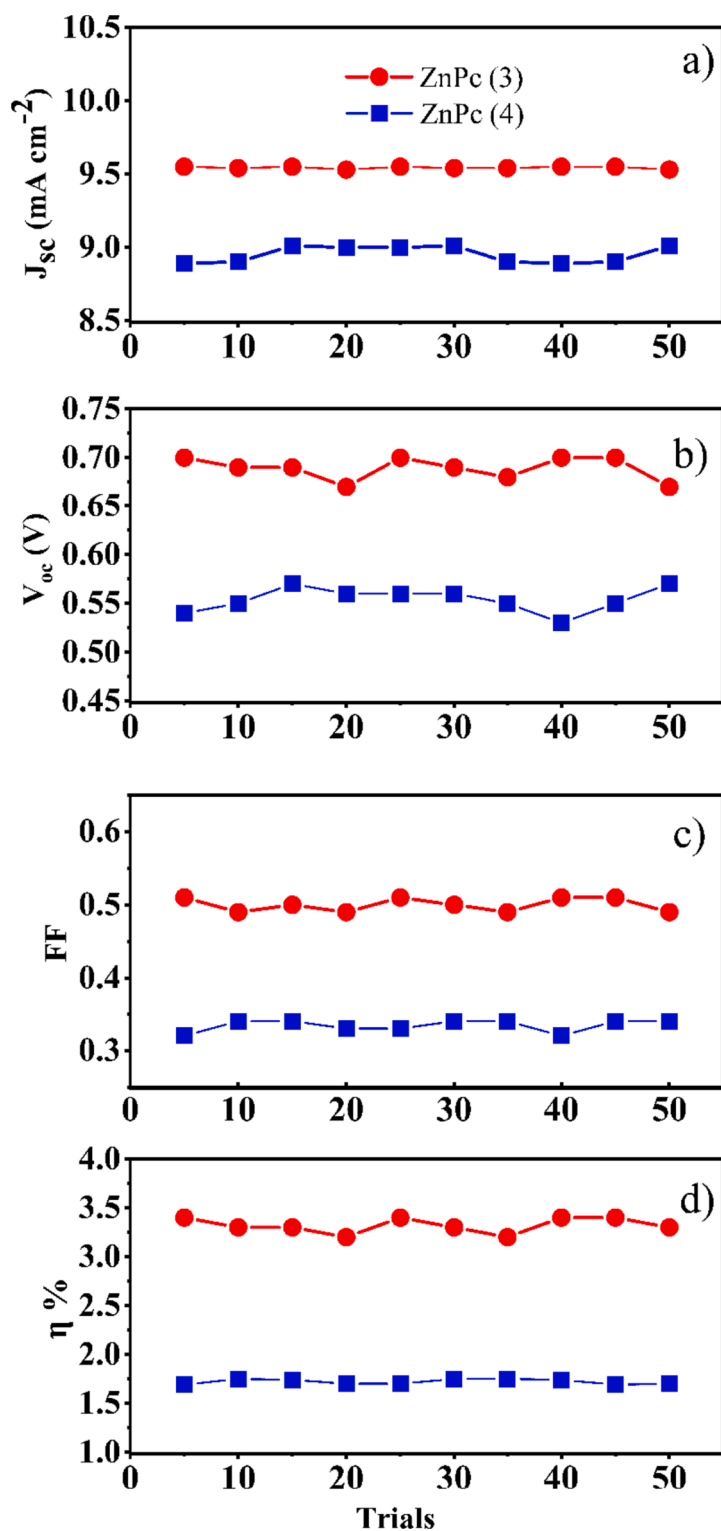


Fig. 9. Long-term stability of ZnPc(3) and ZnPc(4) obtained from 50 LSV trials under 1 sunlight soaking at room temperature. Each photovoltaic performance was measured after a one-hour equilibration time between each J-V measurement.

and a power conversion efficiency (η) of 3.40% values. According to the results of the EIS analysis, which supports the LSV analysis result, ZnPc(3) has a longer electron lifetime of 0.76 ms. These better performance results of the ZnPc(3) can be explained by its asymmetrical structure designed with one naphthoxy and three ethylphenoxy linkers and four carboxy anchoring groups. This molecular design improved electron transfer properties with longer electron lifetimes due to the better

donor-acceptor structure and push-pull effect.

CRediT authorship contribution statement

Gülşah Gümrükçü Köse: Conceptualization, Methodology, Supervision, Investigation, Validation, Formal analysis, Data curation, Visualization, Writing – original draft, Writing – review & editing. **Gülnur**

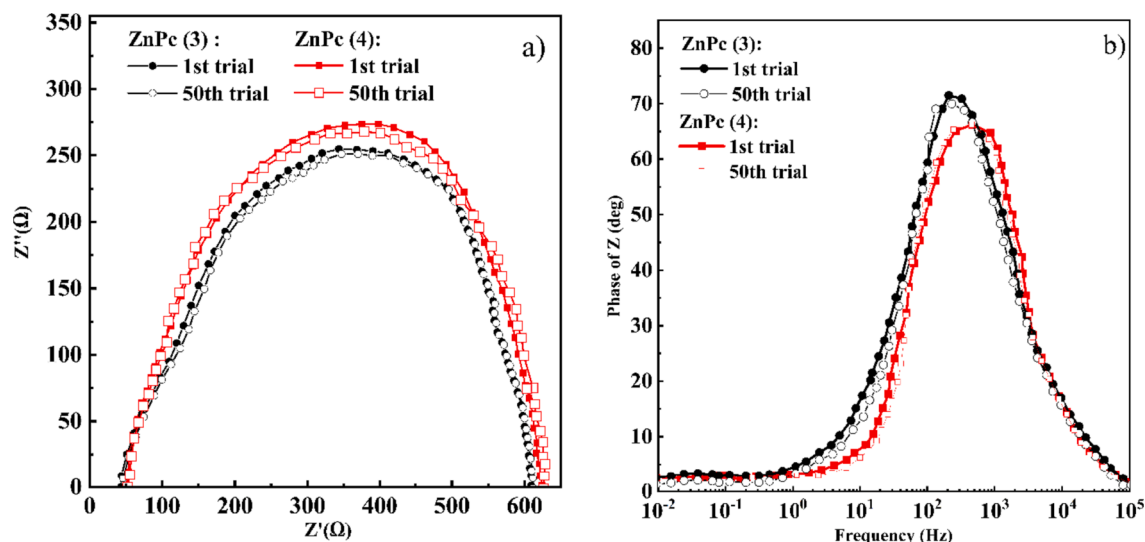


Fig. 10. A) nyquist plots and b) bode plots of ZnPc(3) and ZnPc(4) during the first and 50th cycles under 1 sun light soaking at room temperature.

Keser Karaođlan: Investigation, Validation, Formal analysis, Data curation, Visualization, Writing – original draft, Writing – review & editing. **Yaren Erdađ Maden:** Visualization, Investigation. **Atif Koca:** Conceptualization, Methodology, Supervision, Investigation, Validation, Formal analysis, Data curation, Visualization, Writing – original draft, Writing – review & editing.

Declaration of Competing Interest

The authors declare that they have no known competing financial interests or personal relationships that could have appeared to influence the work reported in this paper.

Acknowledgments

Scientific Research Projects Unit of Marmara University (Project No. FYL-2022-10414).

Atif Koca thanks to Turkish Academy of Sciences (TUBA) for the financial support.

Appendix A. Supplementary data

Supplementary data to this article can be found online at <https://doi.org/10.1016/j.jelechem.2023.117691>.

References

- [1] L. Yu, W. Shi, L. Lin, Y. Liu, R. Li, T. Peng, X. Li, Effects of benzo-annulation of asymmetric phthalocyanine on the photovoltaic performance of dye-sensitized solar cells, *Dalton Trans.* 43 (2014) 8421–8430, <https://doi.org/10.1039/C4DT00411F>.
- [2] M. Urbani, M.E. Ragoussi, M.K. Nazeeruddin, T. Torres, Phthalocyanines for dye-sensitized solar cells, *Coord. Chem. Rev.* 381 (2019) 1–64, <https://doi.org/10.1016/j.ccr.2018.10.007>.
- [3] P.G.V. Sampaio, M.O.A. González, Photovoltaic solar energy: conceptual framework, *Renew. Sustain. Energy Rev.* 74 (2017) 590–601, <https://doi.org/10.1016/j.rser.2017.02.081>.
- [4] A. Yella, H.W. Lee, H.N. Tsao, C. Yi, A.K. Chandiran, M.K. Nazeeruddin, E.W. Diau, C.Y. Yeh, S. Zakeeruddin, M. Grätzel, Porphyrin-sensitized solar cells with cobalt (II/III)-based redox electrolyte exceed 12 percent efficiency, *Sci.* 334 (2011) 629–634, <https://doi.org/10.1126/science.1209688>.
- [5] M.E. Ragoussi, M. Ince, T. Torres, Recent advances in phthalocyanine-based sensitizers for dye-sensitized solar cells, *Eur. J. Org. Chem.* 2013 (2013) 6475–6489, <https://doi.org/10.1002/ejoc.201301009>.
- [6] C.Y. Chen, M. Wang, J.Y. Li, N. Pootrakulchote, L. Alibabaei, C.H. Ngoc-le, J. D. Decoppet, J.H. Tsai, C. Grätzel, C.G. Wu, S.M. Zakeeruddin, M. Grätzel, Highly efficient light-harvesting ruthenium sensitizer for thin-film dye-sensitized solar cells, *ACS Nano* 3 (2009) 3103–3109, <https://doi.org/10.1021/nn900756s>.
- [7] T. Kinoshita, K. Nonomura, N.J. Jeon, F. Giordano, A. Abate, S. Uchida, T. Kubo, S. I. Seok, M.K. Nazeeruddin, A. Hagfeldt, M. Grätzel, H. Segawa, Spectral splitting photovoltaics using perovskite and wideband dye-sensitized solar cells, *Nat. Commun.* 6 (2015) 8834, <https://doi.org/10.1038/ncomms9834>.
- [8] H. Imahori, T. Umeyama, S. Ito, Large π -aromatic molecules as potential sensitizers for highly efficient dye-sensitized solar cells, *Acc. Chem. Res.* 42 (2009) 1809–1818, <https://doi.org/10.1021/ar900034t>.
- [9] X. Li, H. Wang, H. Wu, Phthalocyanines and their analogs applied in dye-sensitized solar cell, in: J. Jiang (Ed.), *Functional Phthalocyanine Molecular Materials*, Springer-Verlag, Berlin, Heidelberg, 2010, pp. 229–273, https://doi.org/10.1007/978-3-642-04752-7_8.
- [10] V.K. Singh, R.K. Kanaparthi, L. Giribabu, Emerging molecular design strategies of unsymmetrical phthalocyanines for dye-sensitized solar cell applications, *RSC Adv.* 4 (2014) 6970–6984, <https://doi.org/10.1039/C3RA45170D>.
- [11] B. Yıldız, B.S. Arslan, E. Güzel, M. Nebiođlu, N. Menges, İ. Şişman, M.K. Şener, Non-aggregating zinc phthalocyanine sensitizer with bulky diphenylphenoxy donor groups and pyrazole-3-carboxylic acid anchoring group for coadsorbent-free dye-sensitized solar cells, *Sol. Energy* 226 (2021) 173–179, <https://doi.org/10.1016/j.solener.2021.08.033>.
- [12] J.J. Cid, J.H. Yum, S.R. Jang, M.K. Nazeeruddin, E. Martínez-Ferrero, E. Palomares, J. Ko, M. Grätzel, T. Torres, Molecular cosensitization for efficient panchromatic dye-sensitized solar cells, *Angew. Chem.* 119 (2007) 8510–8514, <https://doi.org/10.1002/anie.200703106>.
- [13] P.Y. Reddy, L. Giribabu, C. Lyness, H.J. Snaith, C. Vijaykumar, M. Chandrasekharan, M. Lakshmi Kantam, J.H. Yum, K. Kalyanasundaram, M. Grätzel, M.K. Nazeeruddin, Efficient sensitization of nanocrystalline TiO₂ films by a near-IR-absorbing unsymmetrical zinc phthalocyanine, *Angew. Chem.* 119 (2007) 377–380, <https://doi.org/10.1002/ange.200603098>.
- [14] J.J. Cid, M. García-Iglesias, J.H. Yum, A. Forneli, J. Albero, E. Martínez-Ferrero, P. Vázquez, M. Grätzel, M.K. Nazeeruddin, E. Palomares, T. Torres, Structure–function relationships in unsymmetrical zinc phthalocyanines for dye-sensitized solar cells, *Chem. Eur. J.* 15 (2009) 5130–5137, <https://doi.org/10.1002/chem.200801778>.
- [15] S. Eu, T. Katoh, T. Umeyama, Y. Matano, H. Imahori, Synthesis of sterically hindered phthalocyanines and their applications to dye-sensitized solar cells, *Dalton Trans.* 40 (2008) 5476–5483, <https://doi.org/10.1039/B803272F>.
- [16] L. Giribabu, V.K. Singh, T. Jella, Y. Soujanya, A. Amat, F. De Angelis, A. Yella, P. Gao, M.K. Nazeeruddin, Sterically demanded unsymmetrical zinc phthalocyanines for dye-sensitized solar cells, *Dyes Pigm.* 98 (2013) 518–529, <https://doi.org/10.1016/j.dyepig.2013.04.007>.
- [17] G.G. Köse, G.K. Karaođlan, Y.E. Maden, A. Koca, Novel silicon phthalocyanine photosensitizers containing carboxylic acid based axial anchoring groups: electrochemistry, spectroelectrochemistry, and dye sensitized solar cell performance, *Dyes Pigm.* 207 (2022), 110686, <https://doi.org/10.1016/j.dyepig.2022.110686>.
- [18] G.K. Karaođlan, A. Hışır, Y.E. Maden, M.Ö. Karakuş, A. Koca, Synthesis, characterization, electrochemical, spectroelectrochemical and dye-sensitized solar cell properties of phthalocyanines containing carboxylic acid anchoring groups as photosensitizer, *Dyes Pigm.* 204 (2022), 110390, <https://doi.org/10.1016/j.dyepig.2022.110390>.
- [19] Y.E. Maden, G.G. Köse, G.K. Karaođlan, A. Koca, Electrochemical and spectroelectrochemical characterizations of phthalocyanines bearing peripherally tetra-4-carboxyethylenepenoxy anchoring groups and usage as photosensitizers of dye-sensitized solar cell, *J. Electroanal. Chem.* 929 (2023), 117104, <https://doi.org/10.1016/j.jelechem.2022.117104>.

- [20] S. Gorduk, A. Altındal, Peripherally tetra-substituted metallophthalocyanines bearing carboxylic acid groups for efficient dye sensitized solar cells, *J. Mol. Struct.* 1196 (2019) 747–753, <https://doi.org/10.1016/j.molstruc.2019.07.027>.
- [21] C. Ilgün, A.M. Sevim, S. Çakar, M. Özacar, A. Gül, Novel Co and Zn-phthalocyanine dyes with octa-carboxylic acid substituents for DSSCs, *Sol. Energy* 218 (2021) 169–179, <https://doi.org/10.1016/j.solener.2021.02.042>.
- [22] W. Shi, B. Peng, L. Lin, R. Li, J. Zhang, T. Peng, Effect of carboxyl anchoring groups in asymmetric zinc phthalocyanine with large steric hindrance on the dye-sensitized solar cell performance, *Mater. Chem. Phys.* 163 (2015) 348–354, <https://doi.org/10.1016/j.matchemphys.2015.07.049>.
- [23] T. Ikeuchi, H. Nomoto, N. Masaki, M.J. Griffith, S. Mori, M. Kimura, Molecular engineering of zinc phthalocyanine sensitizers for efficient dye-sensitized solar cells, *Chem. Commun.* 50 (2014) 1941–1943, <https://doi.org/10.1039/C3CC47714B>.
- [24] D. Sharma, A. Huijser, J. Savolainen, G. Steen, J.L. Herek, Active and passive control of zinc phthalocyanine photodynamics, *Faraday Discuss.* 163 (2013) 433–445, <https://doi.org/10.1039/C3FD20156B>.
- [25] M.E. Ragoussi, J.J. Cid, J.H. Yum, G. de la Torre, D.D. Censo, M. Grätzel, M. K. Nazeeruddin, T. Torres, Carboxyethyl anchoring ligands: a means to improving the efficiency of phthalocyanine-sensitized solar cells, *Angew. Chem., Int. Ed.* 51 (2012) 4375–4378, <https://doi.org/10.1002/anie.201108963>.
- [26] S.N. Işık, G.K. Karaoğlu, B.C. Ömür, A. Altındal, G.G. Köse, Synthesis, characterization and ethanol sensing properties of carboxylic acid-terminated naphthoxy substituted phthalocyanines, *Synth. Met.* 246 (2018) 7–15, <https://doi.org/10.1016/j.synthmet.2018.09.004>.
- [27] S. Karadağ, C. Bozoğlu, M.K. Şener, A. Koca, Synthesis and electrochemical properties of a double-decker lutetium (III) phthalocyanine bearing electropolymerizable substituents on non-peripheral positions, *Dyes Pigm.* 100 (2014) 168–176, <https://doi.org/10.1016/j.dyepig.2013.09.005>.
- [28] A.W. Snow, 109-Phthalocyanine Aggregation, in: K.M. Kadish, K.M. Smith, R. Guilard (Eds.), *The Porphyrin Handbook: Phthalocyanines: Properties and Materials*, Elsevier Inc., San Diego, California, 2003, pp. 129–176.
- [29] R.D. George, A.W. Snow, J.S. Shirk, W. Barger, The alpha substitution effect on phthalocyanine aggregation, *J. Porphyr. Phthalocyanines* 02 (1998) 1–7, [https://doi.org/10.1002/\(SICI\)1099-1409\(199801/02\)2:1<1::AID-JPP43>3.0.CO;2-L](https://doi.org/10.1002/(SICI)1099-1409(199801/02)2:1<1::AID-JPP43>3.0.CO;2-L).
- [30] P. Matlaba, T. Nyokong, Synthesis, electrochemical and photochemical properties of unsymmetrically substituted zinc phthalocyanine complexes, *Polyhedron* 21 (2002) 2463–2472, [https://doi.org/10.1016/S0277-5387\(02\)01226-3](https://doi.org/10.1016/S0277-5387(02)01226-3).
- [31] A.K. Sarker, M.G. Kang, J.D. Hong, A near-infrared dye for dye-sensitized solar cell: Catecholate-functionalized zinc phthalocyanine, *Dyes Pigm.* 92 (2012) 1160–1165, <https://doi.org/10.1016/j.dyepig.2011.07.002>.
- [32] M. Soltani, R. Minakar, H.R. Memarian, H. Sabzyan, Cyclic voltammetric study of 3, 5-diaryl-1-phenyl-2-pyrazolines, *J. Phys. Chem. A* 123 (2019) 2820–2830, <https://doi.org/10.1021/acs.jpca.9b00642>.
- [33] J.K. Park, H.R. Lee, J. Chen, H. Shinokubo, A. Osuka, D. Kim, Photoelectrochemical properties of doubly β -functionalized porphyrin sensitizers for dye-sensitized nanocrystalline-TiO₂ solar cells, *J. Phys. Chem. C* 112 (2008) 16691–16699, <https://doi.org/10.1021/jp804258q>.
- [34] B. Ameduri, S. Fomin, *Fascinating fluoropolymers and their applications: a volume in progress in fluorine science*, first ed., Elsevier, New York, 2020.
- [35] N. Kobayashi, T. Ashida, T. Osa, Synthesis, spectroscopy, electrochemistry, and spectroelectrochemistry of a zinc phthalocyanine with D_{2h} symmetry, *Chem. Lett.* 21 (1992) 2031–2034, <https://doi.org/10.1246/cl.1992.2031>.
- [36] A. Alemdar, A.R. Özkaya, M. Bulut, Synthesis, spectroscopy, electrochemistry and in situ spectroelectrochemistry of partly halogenated coumarin phthalonitrile and corresponding metal-free, cobalt and zinc phthalocyanines, *Polyhedron* 28 (2009) 3788–3796, <https://doi.org/10.1016/j.poly.2009.07.060>.
- [37] A. Koca, Spectroelectrochemistry of phthalocyanines, in: J.H. Zagal, F. Bedioui (Eds.), *Electrochemistry of N4 macrocyclic metal complexes*, E-Publishing Inc., Switzerland, Springer, 2016, pp. 135–200.
- [38] M.S. Ahmad, A.K. Pandey, N.A. Rahim, Advancements in the development of TiO₂ photoanodes and its fabrication methods for dye sensitized solar cell (DSSC) applications: a review, *Renew. Sustain. Energy Rev.* 77 (2017) 89–108, <https://doi.org/10.1016/j.rser.2017.03.129>.
- [39] M. Garcia-Iglesias, J.H. Yum, R. Humphry-Baker, S.M. Zakeeruddin, P. Péchy, P. Vázquez, E. Palomares, M. Grätzel, M.K. Nazeeruddin, T. Torres, Effect of anchoring groups in zinc phthalocyanine on the dye-sensitized solar cell performance and stability, *Chem. Sci.* 2 (2011) 1145–1150, <https://doi.org/10.1039/C0SC00602E>.
- [40] R. Ghadari, A. Sabri, P.S. Saei, F.T. Kong, H.M. Marques, Phthalocyanine-silver nanoparticle structures for plasmon-enhanced dye-sensitized solar cells, *Sol. Energy* 198 (2020) 283–294, <https://doi.org/10.1016/j.solener.2020.01.053>.
- [41] A.S. Hart, C.B. Kc, H.B. Gobeze, L.R. Sequeira, F. D'Souza, D'Souza, Porphyrin-sensitized solar cells: effect of carboxyl anchor group orientation on the cell performance, *ACS Appl Mater. Interfaces* 5 (11) (2013) 5314–5323.
- [42] J. Xia, N. Masaki, M. Lira-Cantu, Y. Kim, K. Jiang, S. Yanagida, Influence of doped anions on poly (3, 4-ethylenedioxythiophene) as hole conductors for iodine-free solid-state dye-sensitized solar cells, *J. Am. Chem. Soc.* 130 (2008) 1258–1263, <https://doi.org/10.1021/ja075704o>.
- [43] C.G. Claessens, U. Hahn, T. Torres, Phthalocyanines: From outstanding electronic properties to emerging applications, *Chem. Rec.* 8 (2008) 75–97, <https://doi.org/10.1002/tcr.20139>.
- [44] C. Linares-Flores, F. Mendizabal, R. Arratia-Pérez, N. Inostroza, C. Orellana, Substituents role in zinc phthalocyanine derivatives used as dye-sensitized solar cells. A theoretical study using density functional theory, *Chem. Phys. Lett.* 639 (2015) 172–177, <https://doi.org/10.1016/j.cplett.2015.09.025>.
- [45] M. Kimura, H. Nomoto, H. Suzuki, T. Ikeuchi, H. Matsuzaki, T.N. Murakami, A. Furube, N. Masaki, M.J. Griffith, S. Mori, Molecular design rule of phthalocyanine dyes for highly efficient near-IR performance in dye-sensitized solar cells, *Chem. Eur. J.* 19 (2013) 7496–7502, <https://doi.org/10.1002/chem.201300716>.